AGU PUBLICATIONS

Geochemistry, Geophysics, Geosystems

RESEARCH ARTICLE

10.1002/2017GC007169

Lateral Variations in *SKS* Splitting Across the MAGIC Array, Central Appalachians

John C. Aragon[1], Maureen D. Long[1], and Margaret H. Benoit[2]

[1]Department of Geology and Geophysics, Yale University, New Haven, CT, USA, [2]National Science Foundation, Arlington, VA, USA

Key Points:
- We measured *SKS* splitting parameters across the dense MAGIC seismic array in the central Appalachian Mountains
- We document lateral changes in *SKS* splitting and infer that seismic anisotropy in both the lithosphere and asthenosphere is required
- We infer that past episodes of orogenesis and rifting have deformed the lithospheric mantle

Supporting Information:
- Supporting Information S1
- Table S1
- Table S2
- Table S3

Correspondence to:
M. Long,
maureen.long@yale.edu

Citation:
Aragon, J. C., Long, M. D., & Benoit, M. H. (2017). Lateral variations in *SKS* splitting across the MAGIC array, central Appalachians. *Geochemistry, Geophysics, Geosystems*, *18*. https://doi.org/10.1002/2017GC007169

Received 2 AUG 2017
Accepted 27 OCT 2017
Accepted article online 2 NOV 2017

Abstract The eastern margin of North America has been shaped by several cycles of supercontinent assembly. These past episodes of orogenesis and continental rifting have likely deformed the lithosphere, but the extent, style, and geometry of this deformation remain poorly known. Measurements of seismic anisotropy in the upper mantle can shed light on past lithospheric deformation, but may also reveal contributions from present-day mantle flow in the asthenosphere. Here we examine *SKS* waveforms and measure splitting of *SKS* phases recorded by the MAGIC experiment, a dense transect of seismic stations across the central Appalachians. Our measurements constrain small-scale lateral variations in azimuthal anisotropy and reveal distinct regions of upper mantle anisotropy. Stations within the present-day Appalachian Mountains exhibit fast splitting directions roughly parallel to the strike of the mountains and delay times of about 1.0 s. To the west, transverse component waveforms for individual events reveal lateral variability in anisotropic structure. Stations immediately to the east of the mountains exhibit complicated splitting patterns, more null *SKS* arrivals, and a distinct clockwise rotation of fast directions. The observed variability in splitting behavior argues for contributions from both the lithosphere and the asthenospheric mantle. We infer that the sharp lateral transition in splitting behavior at the eastern edge of the Appalachians is controlled by a change in anisotropy in the lithospheric mantle. We hypothesize that beneath the Appalachians, *SKS* splitting reflects lithospheric deformation associated with Appalachian orogenesis, while just to the east this anisotropic signature was modified by Mesozoic rifting.

1. Introduction

The present-day Appalachian Mountains are a result of a Paleozoic accretionary orogen on the eastern margin of Laurentia near the end of a complex Wilson cycle (e.g., Benoit et al., 2014; Cawood & Buchan, 2007; Hatcher, 2010). This cycle began with the breakup of supercontinent Rodinia between ~750 and 550 Ma (e.g., Burton & Southworth, 2010; Li et al., 2008) and the subsequent opening of the Iapetus Ocean. The closing of this ocean completed the Wilson cycle and encompassed the Taconian, Acadian, and Alleghanian orogenies, culminating in the collision of Laurentia and Gondwana to form the supercontinent Pangaea. Later continental rifting, accompanied by magmatic activity of the Central Atlantic Magmatic Province (e.g., McHone, 1996), opened the Atlantic Ocean basin and created the passive continental margin we see today. Our current understanding of the tectonic evolution of eastern North America does much to explain the region's complicated geology, topography, and physiography. Many basic questions remain, however, about the deep structure and dynamics of the eastern North American passive margin—that is, the crust, lithospheric mantle, and asthenosphere. Unsolved problems include the detailed relationships between surface geologic units and lithospheric structure at depth (e.g., Yuan et al., 2014), the extent to which deep structures play a role in controlling intraplate seismicity (e.g., Powell & Thomas, 2016), and the factors influencing the persistence of Appalachian topography (e.g., Miller et al., 2013).

Of particular interest for this study are questions related to the extent, nature, and geometry of continental lithospheric deformation associated with past episodes of orogenesis and rifting (e.g., Barruol et al., 1997), as well as the geometry of present-day flow in the asthenospheric upper mantle and its implications for topographic evolution (e.g., Rowley et al., 2013). In particular, the nature of lithospheric deformation during orogenesis remains a key unsolved problem: the extent to which the mantle lithosphere participates in mountain-building processes, and the geometry of deformation in the deep lithosphere in orogenic systems, remain poorly understood (e.g., Meissner et al., 2002; Tommasi & Vauchez, 2015). Similarly, it is not well known to what extent continental rifting produces large-scale, coherent deformation of large volumes of the mantle lithosphere, and to what extent rifting-related deformation is capable of overprinting existing anisotropic fabric (e.g., Vauchez et al., 2000). The Appalachians represent an excellent locality to test hypotheses about past lithospheric deformation due to orogenesis and rifting, but until recently the availability of broadband seismic data was limited. The advent of EarthScope USArray data set in eastern North America beginning in 2012–2013 has changed this situation dramatically, with both the Transportable Array (TA) and PI-driven Flexible Array experiments enabling transformative studies of deep structure beneath the Appalachians.

Seismic anisotropy, or the directional dependence of seismic wave speeds, represents a key observable for characterizing past and present deformation in the upper mantle. This is because the deformation of mantle rocks in the dislocation creep regime leads to a crystallographic preferred orientation (CPO, also known as lattice preferred orientation or LPO) of individual crystals. For a mantle assemblage dominated by olivine, the relationships between strain and the resulting anisotropy under typical deformation conditions are relatively well known (e.g., Karato et al., 2008). The splitting of shear phases such as *SKS* is a powerful indicator of anisotropy and thus deformation in the Earth's upper mantle (e.g., Long & Silver, 2009). Because it is a core-refracted phase, the initial polarization of an *SKS* wave entering the mantle beneath a station is controlled by the *P*-to-*S* conversion at the core-mantle boundary. This makes the *SKS* phase an ideal choice for measuring seismic anisotropy because the observed splitting is constrained to the receiver side, most likely in the upper mantle (e.g., Long & Silver, 2009), and the initial polarization of the phase matches the backazimuth (that is, the station to event azimuth). When a shear wave propagates through a (weakly) anisotropic medium, it is split into two orthogonally polarized components, and their properties can be measured when ground motion from *SKS* arrivals is recorded by seismic instruments. We measure splitting parameters corresponding to a fast direction (ϕ) and delay time (δt). The fast direction corresponds to the orientation of the fast quasi-*S* phase, and the delay time corresponds to the accumulated delay between the fast and slow components.

Several previous workers have investigated *SKS* splitting beneath eastern North America, including studies based on a relatively small number of stations before the USArray era (e.g., Barruol et al., 1997; Fouch et al., 2000; Levin et al., 1999; Long et al., 2010; Wagner et al., 2012) and more recent studies that have taken advantage of USArray and related experiments (e.g., Gilligan et al., 2016; Long et al., 2016; Yang et al., 2017; White-Gaynor & Nyblade, 2017). Several workers have noted the preponderance of fast directions that strike roughly NE-SW—that is, parallel to the strike of the orogen—at stations located in the Appalachian Mountains (e.g., Barruol et al., 1997; Gilligan et al., 2016; Long et al., 2010, 2016; White-Gaynor & Nyblade, 2017). These observations have often been interpreted as reflecting frozen-in anisotropy in the mantle lithosphere, suggesting that the lithosphere was deformed coherently during orogenesis, as envisioned by the "vertically coherent deformation" model of Silver (1996). However, not all workers have espoused this view; for example, Fouch et al. (2000) and Yang et al. (2017) emphasized present-day flow in the asthenospheric mantle, likely modified by the presence of a thick continental keel, as the major contributor to the observed anisotropy pattern beneath eastern North America. Several studies have pointed out that complex splitting patterns likely require multiple layers of anisotropy (e.g., Darbyshire et al., 2015; Levin et al., 1999; Long et al., 2016), perhaps corresponding to a layer of frozen-in lithospheric anisotropy over a layer of actively deforming asthenosphere. This interpretation is generally consistent with surface wave models that include azimuthal anisotropy, which generally invoke changes in anisotropic geometry with depth beneath eastern North America (e.g., Deschamps et al., 2008; Yuan & Romanowicz, 2010), and with receiver function observations that indicate sharp contrasts in anisotropy with depth (e.g., Yuan & Levin, 2014).

The ambiguity in interpretation of *SKS* splitting measurements beneath eastern North America in terms of past lithospheric deformation, present-day flow in the asthenosphere, or a combination is largely due to limitations of the technique, which has excellent lateral resolution but poor depth resolution. Measurements of *SKS* splitting across dense seismic networks, however, have the potential to resolve detailed variations in anisotropy both laterally and (to a lesser extent) in depth (e.g., Diaz et al., 2010; Long et al., 2009; Polet & Kanamori, 2002; Rümpker et al., 2003; Ryberg et al., 2005), taking advantage of the overlapping Fresnel sensitivity zones for dense array data. Here we present analyses of *SKS* waveforms and splitting parameters at stations of the MAGIC (Mid-Atlantic Geophysical Integrative Collaboration) array, a USArray Flexible Array experiment that deployed 28 broadband stations across the central Appalachians stretching from Charles

City, VA to Paulding, OH (Long & Wiita, 2013). The MAGIC deployment achieved a nominal station spacing of ~25 km, with stations located within the region of highest present-day topography (eastern West Virginia) spaced as closely as ~10–15 km, compared to the nominal spacing of ~70 km for the TA. We obtained ~400 high-quality *SKS* splitting measurements from ~100 teleseismic earthquakes, and also examined in detail record sections from five events with very clear *SKS* arrivals across the array. The measurement and interpretation of splitting parameters across the MAGIC array, combined with the examination of record sections from individual events, give unprecedented resolution of lateral transitions in upper mantle anisotropy across the Appalachian Mountains and insight into how past episodes of orogenesis and rifting have deformed the lithosphere.

2. Data and Methods

Data collection for the MAGIC experiment began in October 2013 with the construction of 13 seismic observatories in Virginia and West Virginia, using Trillium 120PA broadband sensors and Taurus digitizers made by Nanometrics and owned by Yale University. Due to persistent power failures, only seven of the stations operated throughout Year 1 of data collection. In October 2014, the MAGIC experiment received 28 Streckeisen STS-2 broadband sensors and Reftek RT-130 digitizers from the PASSCAL portable seismic instrument pool; this instrumentation was swapped out at existing stations and installed at newly built stations, with the last station installed in October 2015. Run times at individual MAGIC stations thus ranged between 12 and 36 months, with the majority of stations operating for 24 months. The MAGIC station configuration (Figure 1) was a linear array nearly perpendicular to the strike of the Appalachian Mountains, traversing a range of physiographic provinces and surface geologic units. The array was serviced at roughly 6 month intervals and demobilized in October 2016. All data were subjected to standard quality control procedures and archived at the Data Management Center (DMC) of the Incorporated Research Institutions for Seismology (IRIS). We also examined data from permanent station ACSO, located near Columbus, OH, in this study.

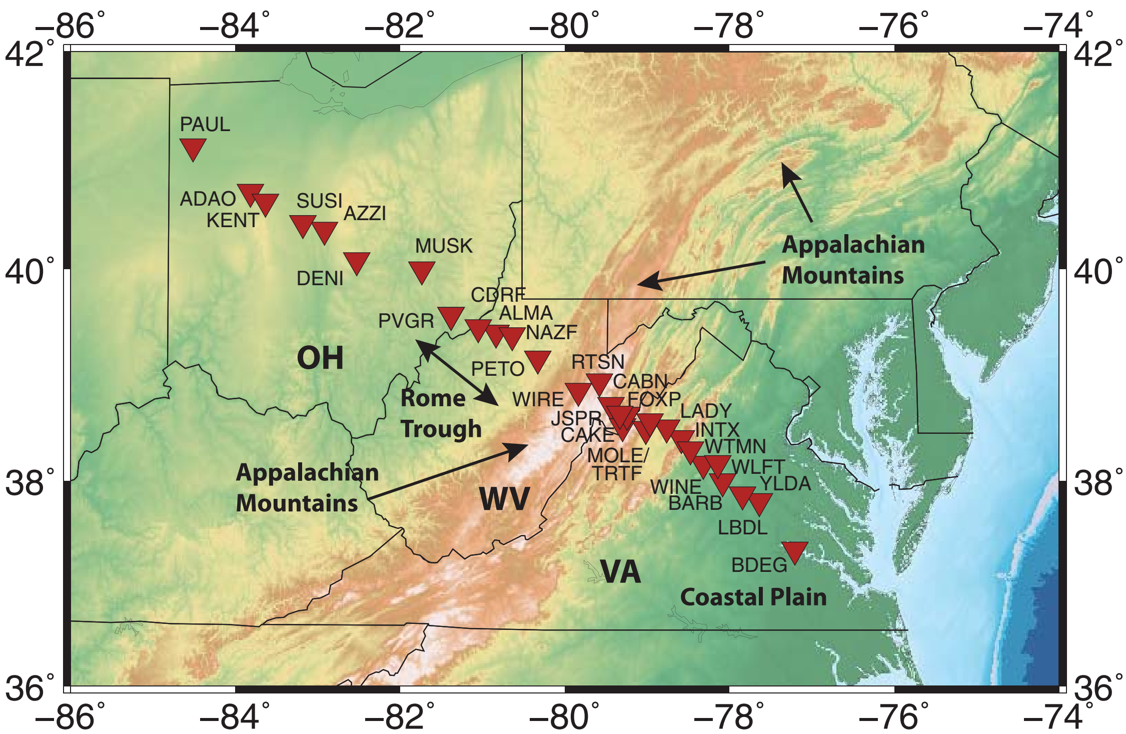

Figure 1. Map of MAGIC station locations (red triangles) across Virginia, West Virginia, and Ohio. (Note that the map shows 29 station locations, instead of 28; stations TRTF and MOLE were nearly colocated, with TRTF operating during Year 2 and MOLE operating during Year 3.) The Appalachian Mountains, Coastal Plain, and Rome Trough are labeled.

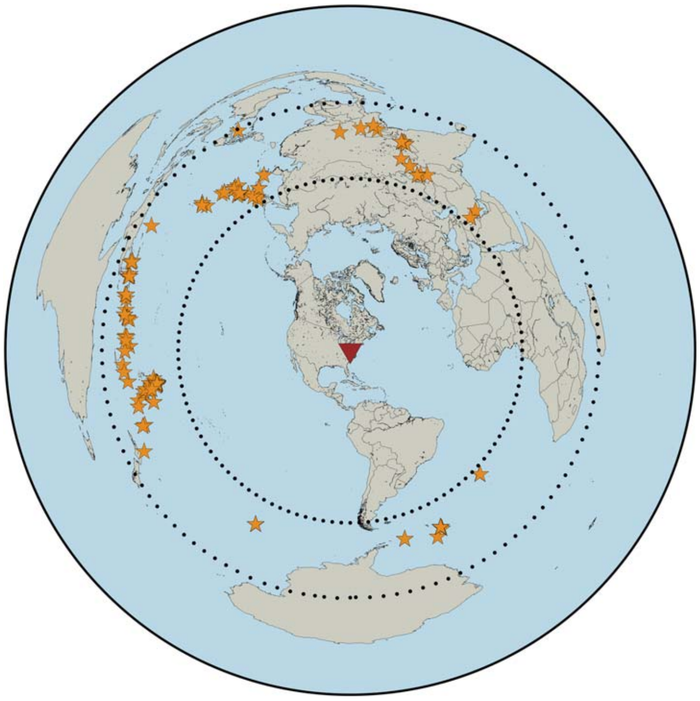

Figure 2. Map of events (stars) used in this study. Each event yielded at least one usable splitting measurement (null or nonnull). Dashed lines show the epicentral distance limits used to select events for analysis (90°–130°).

We used the National Earthquake Information Center (NEIC) catalog to select ∼500 earthquakes of moment magnitude 5.8 or greater at epicentral distances between 90° and 130° from individual stations that occurred during the recording time of the MAGIC experiment. Of these, 105 earthquakes (Figure 2) across a range of backazimuths yielded well-resolved *SKS* parameters for at least one station, as described below. The event map in Figure 2 reveals a limiting factor of sparse backazimuthal coverage between ∼50° and ∼250° due to the distribution of global seismicity, with earthquakes in the western Pacific subduction zones dominating the coverage.

In preparation for splitting analysis, data were bandpass filtered to retain energy at periods between 8 and 25 s, and clear *SKS* arrivals on the radial component were selected. We measured splitting parameters (fast direction, ϕ, and delay time, δt) using the SplitLab software (Wüstefeld et al., 2008), simultaneously applying the rotation-correlation and transverse component minimization methods. Our data preprocessing and splitting analysis procedures followed our previous work in eastern North America (Long et al., 2010, 2016; Wagner et al., 2012), so the results can be compared directly. We retained splitting measurements for which the two methods agreed taking into account the 95% confidence regions (e.g., Long & Silver, 2009); hereinafter we report splitting measurements obtained with the transverse component minimization method (Silver & Chan, 1991). Measurements having 95% confidence regions of up to $\pm15°$ in ϕ and ±0.2 s in δt were marked "good" and those with $\pm25°$ in ϕ and ±0.5 s in δt were marked "fair." Only "good" and "fair" measurements are reported here. *SKS* arrivals with a high signal-to-noise ratio on the radial component, low transverse component noise, and linear uncorrected particle motion were designated as "null" (that is, nonsplit). Null measurements were assigned a quality rating of "good" or "fair" based on the transverse component noise level and the linearity of particle motion, again following our previous work (Long et al., 2010, 2016). Examples of high-quality null and split *SKS* waveforms, along with shear wave splitting diagnostic plots, are shown in Figure 3. Tables of individual splitting measurements, both null and nonnull, can be found in supporting information Tables S1 and S2.

3. Results

Our measurement procedure yielded 405 individual *SKS* measurements at MAGIC stations of "good" or "fair" quality from 105 individual earthquakes. These individual measurements at MAGIC stations are shown in supporting information Tables S1 (nonnull) and S2 (null) and are shown in map view in Figure 4. In the discussion of the results presented here, we combine these 405 new measurements at MAGIC stations with an additional 100 measurements from TA stations located along (or near) the MAGIC line (N49A, O51A, O52A, P52A, P53A, Q55A, R56A, R57A, R58A, R58B, S59A, and T60A). These measurements were previously published by Long et al. (2016) and obtained using the same preprocessing and measurements procedures as the present study. Histograms showing the distribution of individual measurements (null and nonnull) for the combined MAGIC and TA splitting data set along the MAGIC line are shown in Figure 5.

The majority of the measurements in the combined TA and MAGIC data set (70%) were null arrivals, indicating either a lack of anisotropy beneath the station, destructive interference between multiple layers of anisotropy, or an alignment between the initial polarization of the *SKS* phase and the fast or slow direction of the anisotropic medium. The average measured fast direction (modulo 180°) across the MAGIC study region is 67°, with a standard deviation of 25°, and the distribution is bimodal (Figure 5), with peaks around 60° and 105°. In contrast, the measured delay times exhibit a unimodal distribution (Figure 5), with an average δt of 0.92 s (standard deviation 0.25 s). This average delay time is typical for continental regions (e.g., Fouch & Rondenay, 2006; Silver, 1996) and similar to the average for all of eastern North America (Long et al., 2016), but smaller than for the western United States. (e.g., Hongsresawat et al., 2015).

In map view (Figure 4) and in histogram form (Figure 5), it is clear that there are lateral variations in measured splitting parameters as well as in the backazimuthal distribution of null measurements along the MAGIC line. In general, stations in Ohio and West Virginia are dominated by fast splitting directions around 60°, roughly parallel to the strike of the Appalachian range in West Virginia, while average fast directions in Virginia trend more E-W. The distribution of null arrivals (Figure 4b) helps to highlight the possible fast and slow directions associated with anisotropic structure, as well as identify regions of particular complexity. We observe a particularly large number of null arrivals, across a large range of backazimuths, at stations in the eastern portion of the array in central and eastern Virginia. We also observe a large proportion of null arrivals in the western portion of the array, in western Virginia and Ohio. In particular, there is a group of stations

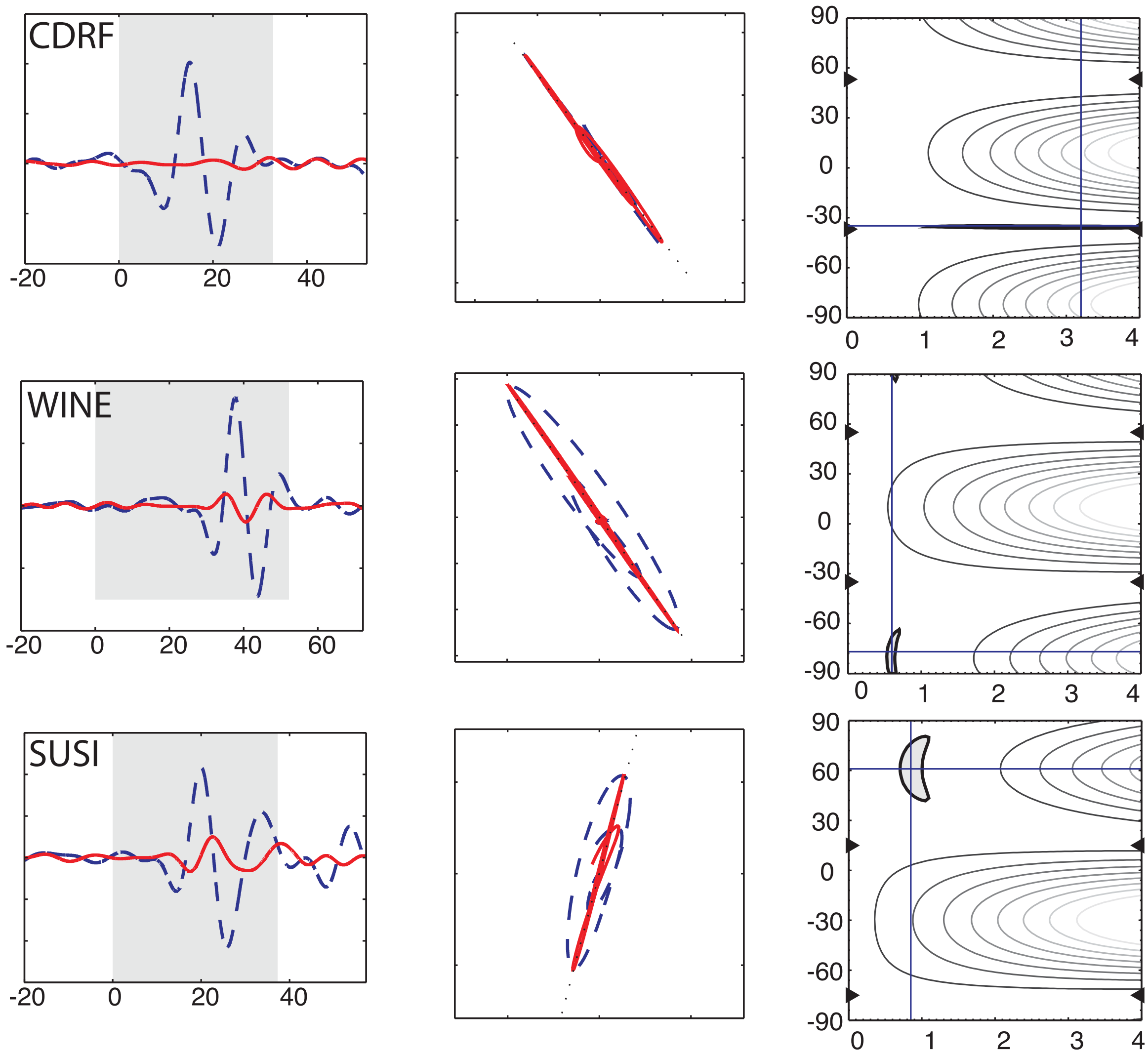

Figure 3. Examples of waveforms and splitting measurements for three *SKS* arrivals at MAGIC stations. (top row) A high-quality null (that is, nonsplit) arrival at station CDRF located to the west of the Appalachians in West Virginia; (middle row) the same event measured at Virginia station WINE, exhibiting weak splitting; bottom row shows a different event measured at Ohio station SUSI, exhibiting slightly stronger splitting with a dramatically different fast direction. (left plots) The radial component waveform (dashed blue line) and the transverse component waveform (solid red line), with the time window used in the splitting analysis shaded in gray. (middle plots) Particle motion diagrams for the *SKS* arrival in map view, with north pointing up; the dashed blue line shows the uncorrected particle motion, while the solid red line shows the particle motion after the effect of splitting has been removed. (right plots) Diagnostic plots and 95% error estimates (gray region) for the transverse component minimization measurement method, with the delay times shown on the *x* axis and the fast directions on the *y* axis. Crossed lines indicate the best-fitting pair of splitting parameters for each arrival.

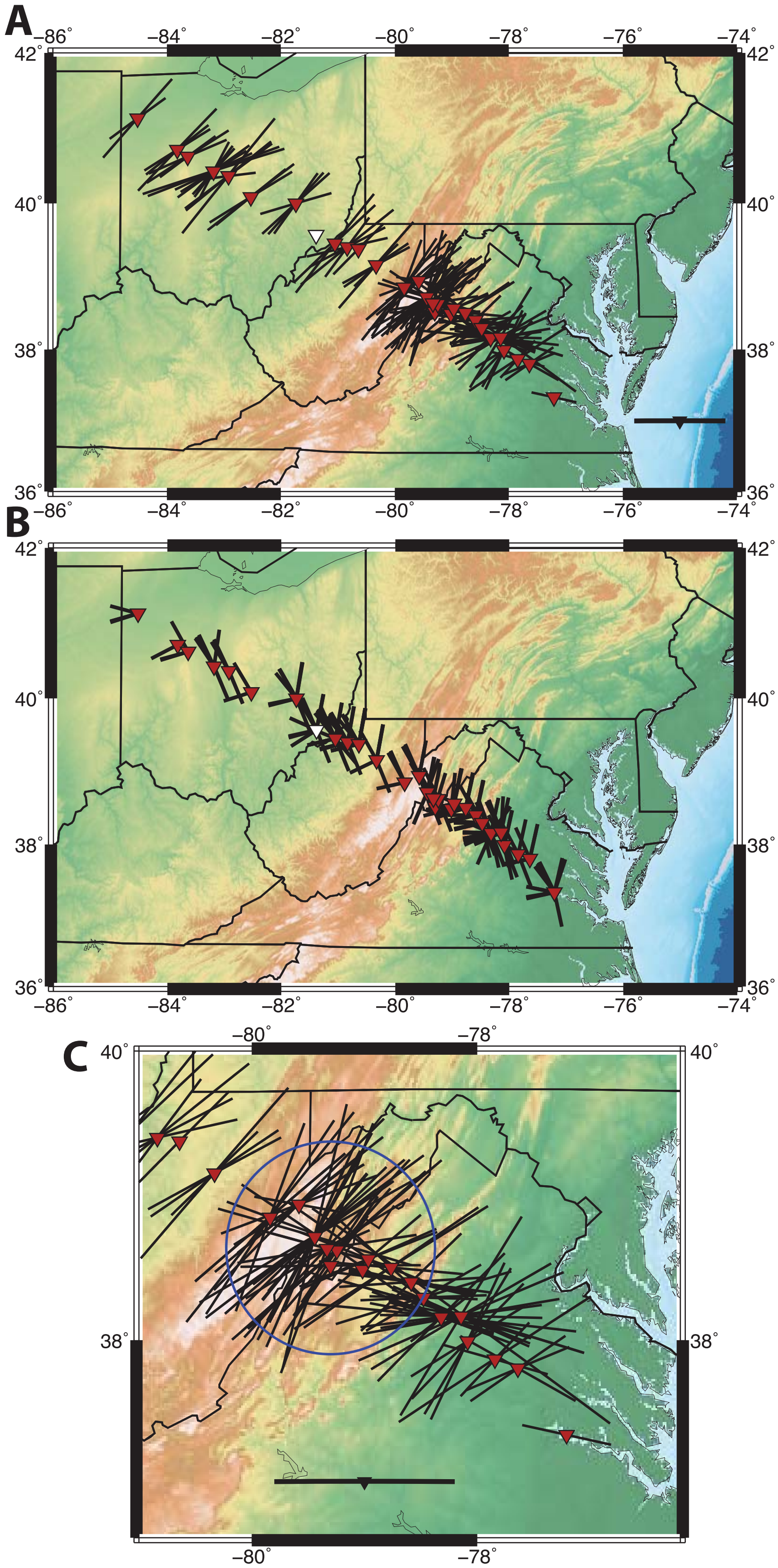

Figure 4. (continued)

in western West Virginia and southeastern Ohio that are dominated by null arrivals, including one (PVGR) at which we recorded only null arrivals across all backazimuths, with no clearly split *SKS* phases.

The patterns visible in map view in Figure 4 suggest a grouping of MAGIC (and TA) stations into three regions, each with its own general splitting characteristics. Stations in the "western" region (PAUL, N49A, ADAO, KENT, SUSI, ACSO, AZZI, O51A, DENI, P52A, O52A, MUSK, P53A, PVGR, CDRF, ALMA, NAZF, PETO, and Q55A) are situated in the generally flat topography of the Central Lowland province of Ohio or the rolling hills of the Appalachian Plateau, covering eastern Ohio and the western half of West Virginia. This group of stations exhibits a consistent orientation of measured ϕ, with a unimodal distribution around 60° (Figure 5), and a high proportion of null measurements (77%). A group of stations that we designate as "mountain" stations (WIRE, RTSN, CABN, R56A, JSPR, CAKE, and FOXP) are located in the high topography of the Valley and Ridge province of eastern West Virginia. We obtained a much lower proportion of null measurements at mountain stations (40%) relative to the rest of the array, even though the backazimuthal coverage is similar. A histogram of measured fast directions at mountain stations (Figure 5) shows a bimodal distribution, with a peak around 60° (similar to the dominant fast direction for the western stations) and a smaller peak around 100°. Finally, stations in Virginia, which we designate as the "eastern" region (MOLE/TRTF, LADY, INTX, R57A, WTMN, WINE, WLFT, BARB, R58A, R58B, YLDA, LBDL, S59A, BDEG, and T60A), traverse the Blue Ridge, Piedmont, and Coastal Plain provinces. These stations yield a high proportion of null *SKS* arrivals (74%), and their measured ϕ values (Figure 5) exhibit a bimodal distribution with a main peak around 110° and a secondary peak around 60°. We did not observe any major differences in measured delay times among the western, mountain, and eastern groups of stations, although average delay times are slightly higher in the mountain stations (0.98 s) than in the western (0.92 s) or eastern (0.86 s) regions.

Another way of viewing the individual measurements in our data set is to plot splitting measurements for each station as a function of backazimuth and incidence angle (nearly constant and close to vertical for *SKS* phases) on a stereographic projection. Such stereoplots are a particularly useful way of visualizing variations in apparent splitting with backazimuth, which indicate lateral and/or vertical variations in anisotropy (e.g., Levin et al., 1999; Silver & Savage, 1994; Yuan & Levin, 2014). Figure 6 shows representative stereoplots for MAGIC stations in the western, mountain, and eastern regions, ordered from west to east, illustrating the range of splitting behavior across the array. (A complete set of stereoplots for MAGIC stations, as well as TA stations located along the MAGIC line, is shown in supporting information Figure S1.) At western stations (top row in Figure 6), we observe generally relatively simple splitting patterns with little azimuthal variability, and one station that notably exhibits only null measurements (PVGR). At mountain stations (middle row in Figure 6), splitting patterns are somewhat more complex; they are dominated by nearly orogen-parallel ϕ and fewer null measurements, with some backazimuthal variability and a few nearly E-W fast directions at each station. At eastern stations (bottom row in Figure 6), the splitting patterns are complex, with more dramatic variations in apparent splitting, a mix of null and split arrivals (often at similar backazimuths), and a higher proportion of nearly E-W fast directions.

In addition to the splitting measurements, the *SKS* waveforms themselves yield insight into lateral variability of upper mantle structure when examined along a dense array. In order to facilitate a detailed examination of transverse component waveforms across the array, we selected five earthquakes across a range of backazimuths with clear radial component *SKS* arrivals. Horizontal component waveforms were filtered to retain energy between 8 and 25 s periods, rotated to their radial and transverse components, aligned on the predicted *SKS* arrival time from the iasp91 Earth model (Kennett & Engdahl, 1991), and plotted as a function of

Figure 4. *SKS* splitting measurements at MAGIC stations. (a) A map of individual nonnull *SKS* splitting measurements made using the transverse component minimization method, plotted at the station locations (triangles) is shown. The orientation of each bar shows the fast splitting direction, while its length indicates the delay time. The scale bar in the lower right indicates a delay time of 1 s. The white triangle indicates station PVGR, which recorded only null measurements. (b) Documents null *SKS* arrivals; the orientations of the bars indicate the backazimuth of each null arrival. (c) The same map as in Figure 4a, zoomed in on the area surrounding western Virginia, to show the details of the transition in splitting behavior between stations in the Appalachian Mountains and stations to the east. Plotting conventions are as in Figure 4a. In Figure 4c, the blue ellipse indicates the approximate region that is associated with low seismic velocities at depths of $\sim$100 km in the upper mantle (e.g., Schmandt & Lin, 2014) and with possible lithospheric loss or delamination (e.g., Evans et al., 2016; Mazza et al., 2014).

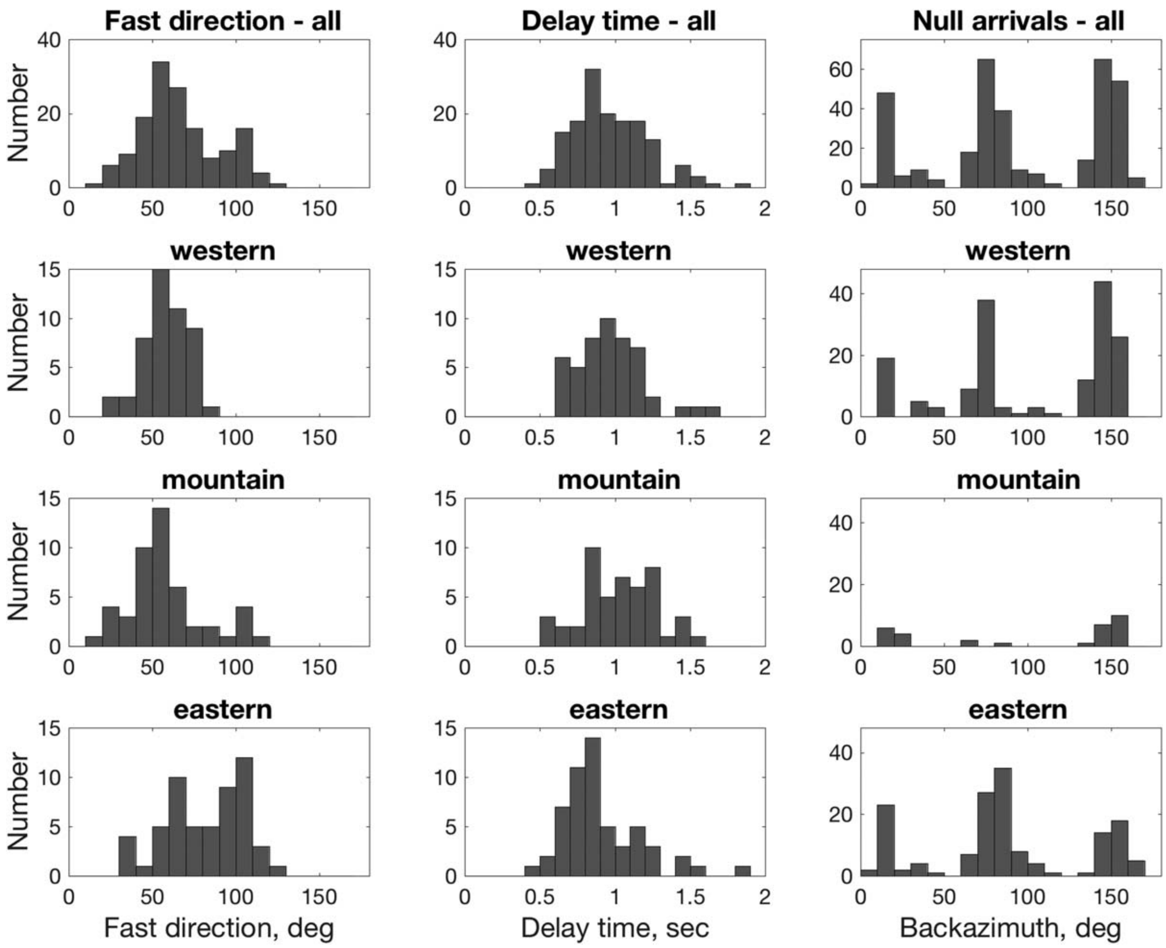

Figure 5. Histograms of the distribution of individual splitting measurements at stations along the MAGIC line, including both MAGIC stations (this study) and TA stations (measurements from Long et al., 2016). (top row) Histograms for all stations, including (left) measured fast directions, (middle) measured delay times, and (right) backazimuths of null (nonsplit) *SKS* arrivals. In the second through fourth rows, the stations are divided by region, with western stations in the second row, mountain stations in the third row, and eastern stations in the bottom row. In rows 2–4, the axes on the histogram plots have been standardized for straightforward visual comparison.

epicentral distance from the source. One such record section is shown in Figure 7; additional record sections are shown in supporting information Figures S2–S5.

The waveforms shown in Figure 7, for an earthquake in the Mariana subduction zone with phases arriving roughly from the northwest, demonstrate lateral variability for the transverse components and yield important clues to the upper mantle structure. We note, first, that radial component *SKS* arrivals are delayed by several seconds in the eastern portion of the array relative to the westernmost stations, likely reflecting a previously documented low velocity anomaly in the upper mantle beneath the central Appalachians (e.g., Schmandt & Lin, 2014). (The approximate location of this low-velocity anomaly is indicated on Figure 4c.) The transverse component waveforms reflect the splitting of the *SKS* phase. In the absence of splitting, they should display zero energy, but when the wave has undergone splitting, they will take the shape of the time derivative of the radial component multiplied by a scalar quantity known as the splitting intensity (Chevrot, 2000). The splitting intensity varies as a function of $\delta t \sin 2\beta$, where β is the angle between the initial polarization direction of the shear wave (equivalent to the backazimuth for *SKS* phases) and the fast direction ϕ. The transverse component amplitude is therefore maximized when δt is large, and/or when the angle between ϕ and the backazimuth is close to 45°. Detailed examination of transverse component waveforms in record section is particularly useful for the MAGIC data set because of the large number of *SKS* arrivals with weak but nonzero transverse component amplitudes (so-called "near null" measurements); traditional splitting measurement methods cannot reliably estimate splitting in this case (e.g., Long & Silver,

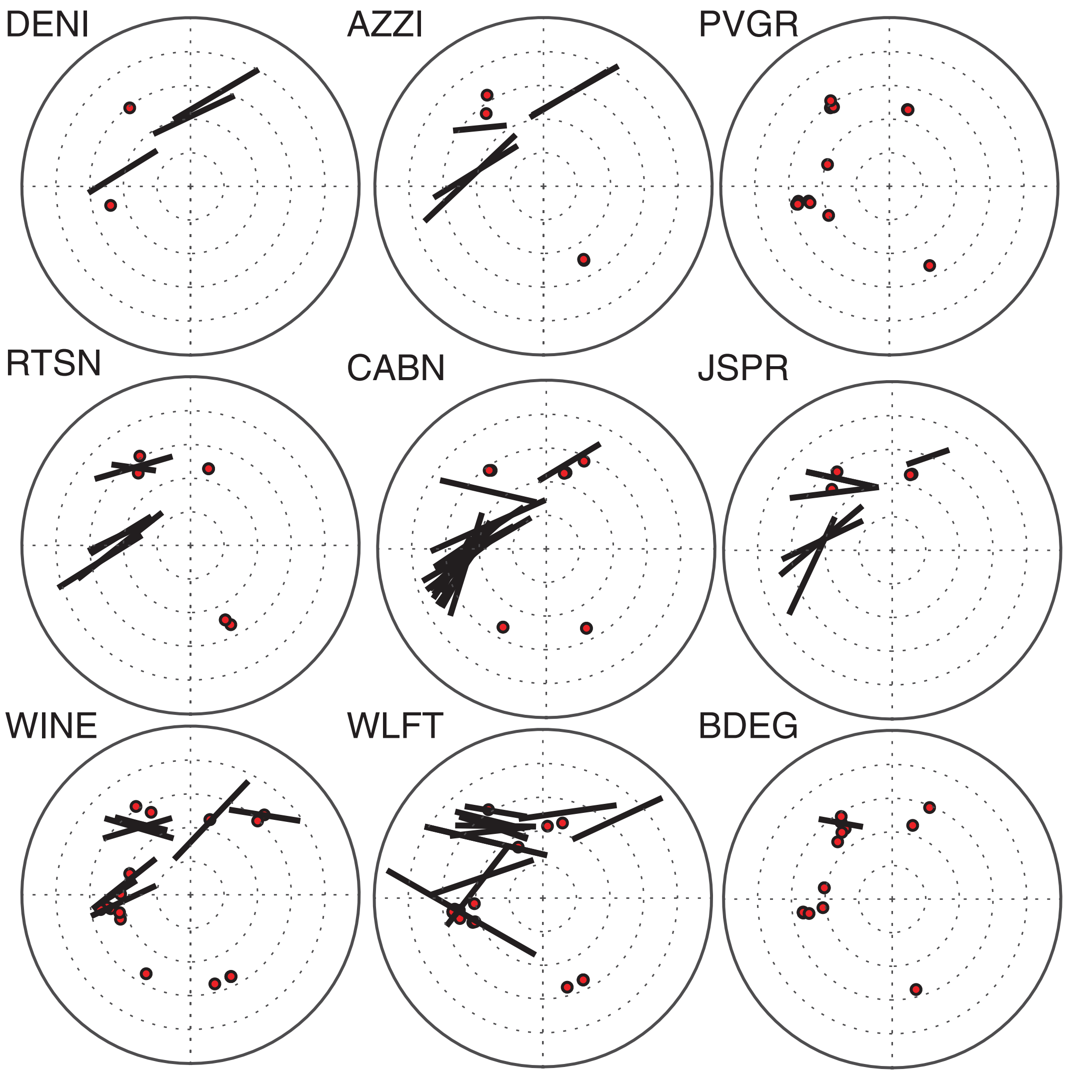

Figure 6. Examples of stereoplots showing *SKS* splitting measurements (as a function of backazimuth and incidence angle) at individual MAGIC stations, with bars showing split measurements and red dots indicating null measurements. (top row) Stations located in the western part of the array (DENI, AZZI, and PVGR), (middle row) stations located in the Appalachian Mountains (RTSN, CABN, and JSPR), and (bottom row) stations located in the eastern part of the array (WINE, WLFT, and BDEG). Stereoplots for all MAGIC stations are shown in supporting information Figure S1.

2009). This means that many of the waveforms shown in Figure 7 do not have corresponding splitting measurements in supporting information Tables S1 and S2 or in Figures 4 and 5; for the case of weak or "near null" measurements, we can visualize the weak transverse component energy in record section view but cannot reliably constrain a "good" or "fair" set of splitting parameters via the measurement methodologies used in this paper.

The record section in Figure 7 clearly illuminates variability in splitting along the MAGIC array for this particular *SKS* arrival. The stations that we designate as "mountain" stations in eastern West Virginia, along with the westernmost Virginia stations, exhibit very similar transverse component waveforms (and thus similar splitting), while the amplitude of the transverse component diminishes to the east, and the easternmost station (BDEG) exhibits nearly linear particle motion. In western West Virginia and Ohio, there is a great deal of variability in the transverse component waveforms, suggesting lateral heterogeneity in splitting behavior within this region. This inferred lateral variability is less obvious from the map view of the entire data set in Figure 4, but clearly expresses itself in the waveforms themselves. Similar geographic patterns are also visible in the transverse component record sections in supporting information Figures S2–S5, which show

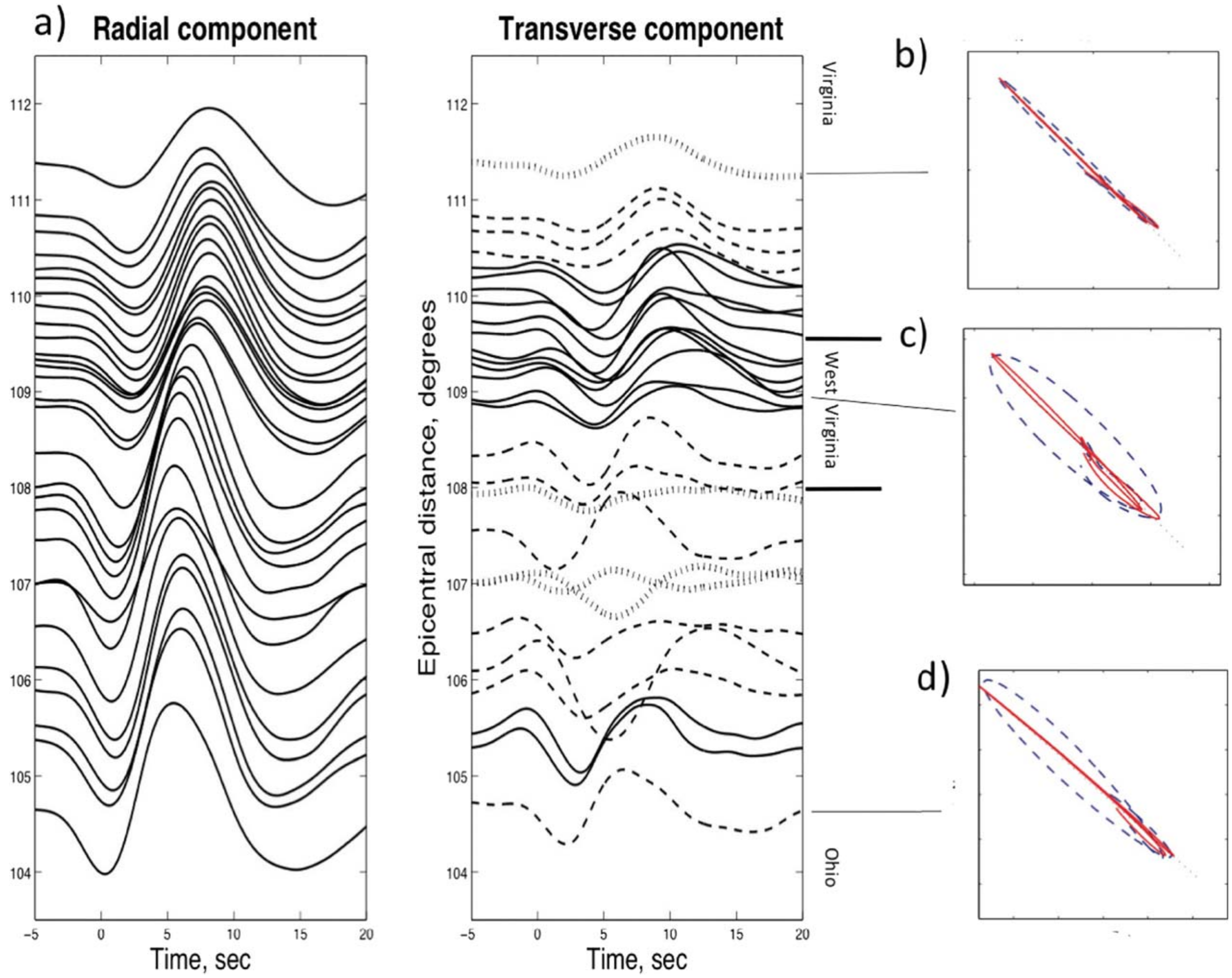

Figure 7. Record section for an *SKS* arrival at MAGIC and selected Transportable Array stations from an event originating from the Northern Mariana Islands on 29 July 2016 ($M_W = 7.7$, depth = 196 km, average backazimiuth = 314°). (a) The radial component waveforms on the left and transverse component waveforms (amplitudes multiplied by 2 to show detail) on the right, plotted as a function of epicentral distance. Transverse component plotting convention corresponds to the character of the splitting behavior for this arrival, with null arrivals shown with dotted lines, weakly split arrivals shown with dashed lines, and clearly split arrivals with solid lines. Note similarity of the waveform behavior for the group of stations located in the Appalachian Mountains (near Virginia-West Virginia border). (b–d) Particle motion diagrams demonstrating characteristic splitting behavior for this event for each region, with (b) a nearly null arrival in the eastern part of the array, (c) a split arrival in the Appalachian Mountains, and (d) a weakly split arrival in the western part of the array. Additional examples of record sections are shown in supporting information Figures S2–S5.

phases arriving from a range of backazimuths. The actual behavior of the waveforms varies greatly among the different events (recall that the transverse component amplitude is a nonlinear function of the phase backazimuth, the delay time, and the fast direction). For each event, however, there is variability in splitting intensity across the array, particularly within the eastern and western groups of stations. In each case, the mountain stations typically have very similar waveforms, suggesting that they are sampling a coherent region of anisotropy that is distinct from the more complex and laterally variable eastern and western regions.

4. Discussion

4.1. Three Distinct Regions of Anisotropic Structure

From the *SKS* measurements shown in Figures 4–6, as well as the record sections presented in Figure 7 and supporting information Figures S2–S5, we infer that there are three distinct regions of upper mantle anisotropy beneath the MAGIC study area. In the eastern portion of the array, anisotropy is complex, with slightly smaller than average delay times, a preponderance of null *SKS* arrivals, and generally nearly E-W fast splitting directions (Figure 5). At eastern stations, we observe pronounced variability in splitting behavior with backazimuth (Figure 6), suggesting lateral and/or vertical heterogeneity in anisotropic structure. Beneath the mountain stations, located in the region of present-day high topography in eastern West Virginia, we observe a substantially smaller proportion of null arrivals than elsewhere in the array, along with dominantly NE-SW fast directions and similar transverse component waveform behavior for individual *SKS* phases (Figure 7). The easternmost stations in the mountain group show a few measurements with nearly E-W ϕ, suggesting that they may be sampling the transition from NE-SW fast directions beneath the Appalachian Mountains to more E-W fast directions just to the east. Finally, beneath the western portion of the array, the average measured fast directions are similar to those at the mountain stations; however, the higher proportion of null arrivals and the distinct lateral variability in transverse component waveforms (Figure 7) suggest that there is significant lateral heterogeneity in anisotropy within this region.

Figure 8 shows single-station average splitting parameters at both MAGIC and TA stations; average (ϕ, δt) measurements for each MAGIC station are also shown in supporting information Table S3. Although a single-station averaging approach obscures the complexity evident in the splitting patterns (Figure 6), it provides a basis for a first-order comparison between the new measurements presented in this study and the previously published TA measurements of Long et al. (2016). In the western portion of the array, our measured fast directions and delay times are generally consistent with previous measurements at TA stations in the region. Notably, our finding of null *SKS* arrivals across a range of backazimuths at station PVGR in southeastern Ohio is consistent with the findings of Long et al. (2016) for nearby TA station P53A, supporting our inference of weak and/or highly heterogeneous anisotropy beneath a localized area, despite the coherent splitting observed at surrounding stations (Figure 8). Beneath the Appalachian Mountains, results from MAGIC agree very well with previous results at TA stations, with nearly identical average ϕ values (58° for MAGIC versus 61° for TA). Our inference of a distinct and coherent splitting signal beneath the central Appalachians is consistent with the major findings of Long et al. (2016), who emphasized the uniformly orogen-parallel fast directions observed throughout the southern and central Appalachian Mountains, including the bend around the Pennsylvania Salient (Figure 8; see also White-Gaynor & Nyblade, 2017).

Beneath the eastern portion of the MAGIC study area, a comparison between our measurements and previous measurements for the TA sheds new light on the complexity of upper mantle anisotropy beneath the Atlantic Coastal Plain. The work of Long et al. (2016) emphasized the dominance of null *SKS* arrivals across the southeastern U.S. Coastal Plain, confirming results from earlier papers (Long et al., 2010; Wagner et al., 2012). Long et al. (2016) suggested that the region of dominantly null splitting may extend as far north as Virginia; however, the results obtained from the MAGIC array show that splitting patterns in central and eastern Virginia are complex, with a mix of null and split arrivals and variability in measured fast directions. Our inference of complex and variable upper mantle anisotropy beneath much of Virginia from MAGIC observations may extend to other regions of the southeastern U.S. as well, and may help explain discrepancies in published *SKS* splitting data sets for this region (Long et al., 2016; Yang et al., 2017) for studies that have used different frequency contents, preprocessing techniques, and measurement methods.

4.2. Evidence for Multiple Layers of Anisotropy

Overall, the complexity in the individual station stereoplots in Figure 6 suggests the presence of multiple layers of anisotropy throughout our study region, particularly in the eastern portion of the array. This, in turn, suggests that there are generally contributions to *SKS* splitting from both lithospheric and asthenospheric mantle beneath the central Appalachians. This inference is consistent with the evidence for both lithospheric and asthenospheric anisotropy beneath much of continental North America inferred from *SKS* splitting and other anisotropy measurements (e.g., Buehler & Shearer, 2017; Darbyshire et al., 2015; Deschamps et al., 2008; Hongsresawat et al., 2015; Long et al., 2016; Yuan & Levin, 2014; Yuan & Romanowicz, 2010). If present-day deformation of the asthenospheric mantle is due to simple shear between the North American plate and the underlying asthenosphere, then we would expect contributions to splitting from a layer with a generally NE-SW fast direction; this is similar to the overall average ϕ that we measure beneath MAGIC. We emphasize, however, that plate motion parallel shear in the asthenosphere cannot explain the lateral transitions in splitting behavior over short length scales that we see. We therefore suggest that our measurements can best be explained by a combination of present-day asthenospheric flow and complex lithospheric anisotropy that varies laterally (and perhaps vertically). The presence of multiple

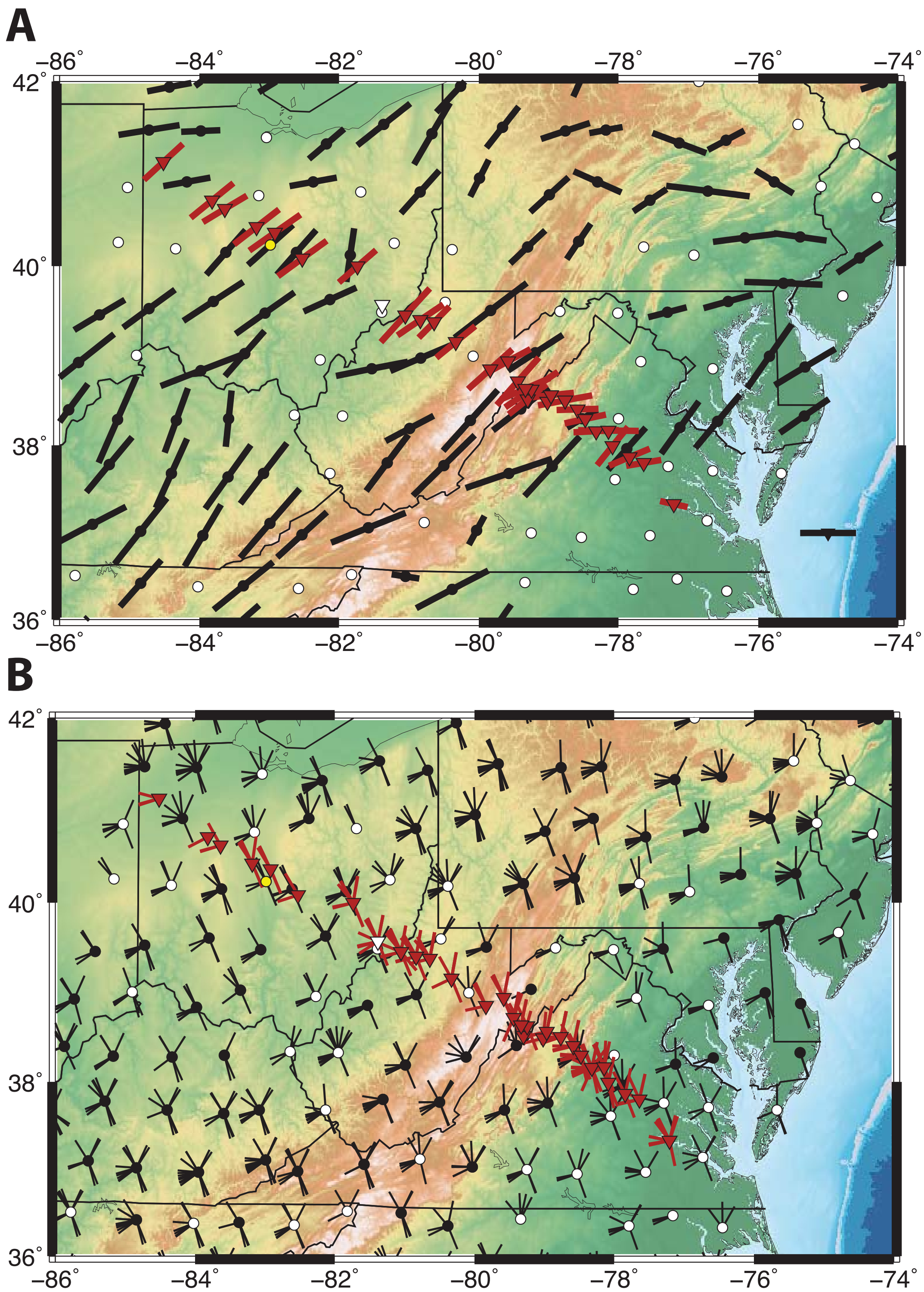

Figure 8. (a) Single-station average splitting parameters and (b) backazimuthal distribution of null measurements at MAGIC and TA stations along the MAGIC line. Permanent station ACSO is shown with a yellow circle. In Figure 8a, red bars indicate average splitting parameters at MAGIC stations, while black bars indicate average splitting beneath TA stations from Long et al. (2016). White circles (TA) and triangles (MAGIC) show stations that exhibit well-resolved null arrivals over a range of backazimuths, with no well-constrained split measurements. In Figure 8b, bars indicate the backazimuth of each nonsplit *SKS* arrival; measurements in red at MAGIC stations are from this study, while measurements in black at TA stations are from Long et al. (2016). The scale bar at bottom right indicates a delay time of 1 s.

anisotropic layers likely results in various degrees of constructive and destructive interference beneath different portions of the array to produce the complicated splitting patterns that we observe.

In order to test the hypothesis of multiple layers of anisotropy beneath much of our study region, we construct plots of individual splitting measurements as a function of backazimuth to determine whether there are clear 90° periodicities in the observations, as would be expected for multiple layers of anisotropy (e.g., Silver & Savage, 1994). The relatively short period of deployment of both the TA and the MAGIC stations means that individual stations do not generally have sufficient backazimuthal coverage to identify clear patterns; therefore, we plot observations for stations within each group (western, mountain, and eastern) together. Figure 9 demonstrates the backazimuthal variability of null and nonnull measurements in the combined MAGIC and TA data set. Evidence for some backazimuthal variability in measured fast direction is clear in each of the three subregions. In the mountain and eastern regions, there is clear evidence for a roughly 90° periodicity in measured fast directions. Specifically, beneath the mountain stations, there is a clear clockwise rotation in measured fast directions with increasing backazimuth in the backazimuthal range between roughly 75° and 145°. Beneath the eastern stations, there is a similar clockwise rotation in ϕ values in the backazimuthal range between roughly 90° and 150°, with a similar rotation in the backazimuthal range between roughly 10° and 45°. Beneath the western stations, in contrast, this strong variability consistent with a 90° periodicity is not evident; while there is some hint of a progressive rotation in ϕ, a periodic pattern is not as clear as in the mountain and eastern regions. In the western portion of the array, the weak backazimuthal variability may reflect lateral heterogeneity in anisotropic structure within the region, as demonstrated in the record section in Figure 7, rather than making an argument for multiple layers. In all three regions, some variability in measured δt values is evident, but it is difficult to discern a clear periodicity or pattern with backazimuth.

At first glance, the character of the backazimuthal variability between the mountain stations and eastern stations in Figure 9 looks similar, although the data are more scattered in the east (and include more split and null measurements from similar backazimuths). Upon closer inspection, however, it is evident that the details of the patterns are different, arguing that the parameters describing the multiple anisotropic layers must change between the mountain and eastern regions. Specifically, the splitting behavior for SKS phases arriving from a backazimuth of $\sim$80°, a direction that is well represented in the data sets for both regions, is strikingly dissimilar. Beneath the mountains, there is a large group of well-resolved splitting measurements with ϕ values around 45°, while beneath the eastern stations, this set of measurements are nearly all null arrivals, with a few (conflicting) nonnull measurements. The two regions exhibit different behavior at backazimuths around 140–150° as well; a majority of the null measurements in the mountain region arrive from this backazimuthal range, mixed in with some split measurements, while in the eastern region there is a much higher proportion of well-resolved, tightly clustered nonnull measurements. Finally, there is a difference in the backazimuthal range between 10° and 45°: beneath the mountains, there are only a few measurements (a mix between split and null) with no clear dependence on backazimuth, while beneath the eastern region, there is a suggestion of a clockwise rotation with increasing backazimuth.

In order to explore whether a change in a two-layer anisotropic model can plausibly explain the difference in the fast direction variability between the mountain and eastern stations, we carry out a highly simplified forward modeling exercise using the analytical equations for multiple-layer apparent splitting of Silver and Savage (1994), as implemented in the MSAT toolkit of Walker and Wookey (2012). This type of forward modeling is decidedly nonunique and is not intended to be exhaustive, as several of the key assumptions made in this type of forward modeling approach are likely to be violated by our observations. Specifically, this modeling approach ignores finite frequency effects (discussed further below), which are likely to be important for stations near the boundary between the two regions, and also makes the assumption of lateral heterogeneity within each region, which does not strictly hold, given the waveform observations in Figure 7 and supporting information Figures S2–S5. These simple models can, however, demonstrate whether a change in anisotropic parameters for a two-layer model can reproduce at least some aspects (if not the details) of the backazimuthal variations evident in Figure 9. We first identified a best-fitting two-layer model for the mountain stations by carrying out a grid search in 5° and 0.1 s increments for (ϕ, δt) in the upper and lower layers, and identifying the model with the minimum root-mean-square (L2) misfit to the (nonnull) measured apparent fast directions in Figure 9. Because the apparent delay times do not display clear periodic trends, we do not use them to identify the best-fitting model. The grid search yielded best-fitting

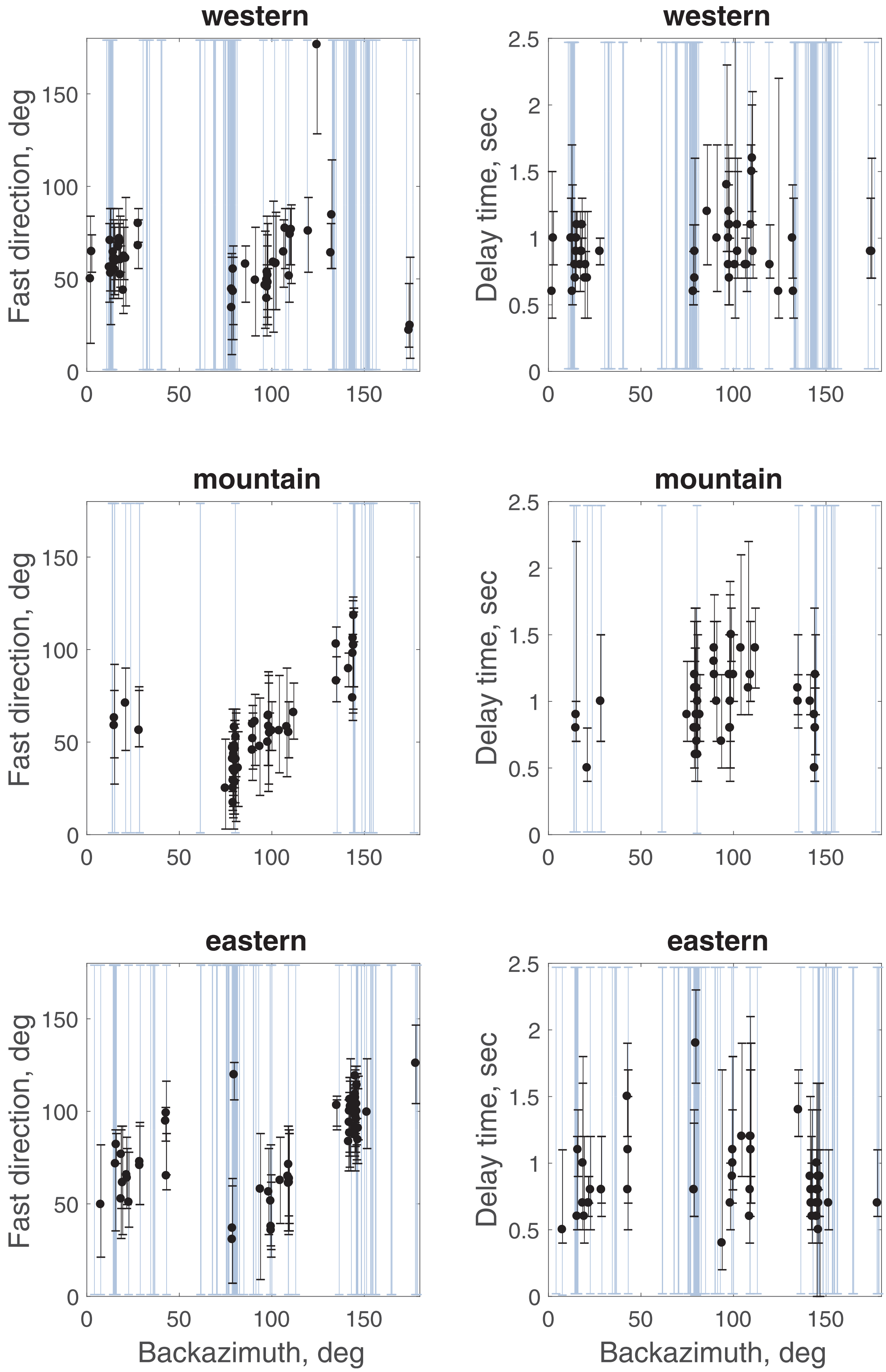

Figure 9. (continued)

model parameters of (80°, 0.9 s) for the lower (asthenospheric) layer, and (40°, 0.3 s) for the upper (lithospheric) layer. A comparison between these best-fitting two-layer model predictions and the observations are shown in Figure 10 (top row). Encouragingly, these parameters are reasonable, as the fast direction for the lower layer is within 10° of the absolute plate motion in the HS3-Nuvel1A plate motion model (Gripp & Gordon, 2002). Similarly, the nearly NE-SW fast direction inferred in for the lithospheric layer is close to the strike of the Appalachian Mountains. The two-layer model, however, is only partially successful at fitting the observations beneath mountain stations (Figure 10). It correctly reproduces the clockwise rotation over backazimuths between roughly 75° and 120°, but does not correctly predict the more nearly E-W fast directions arriving from backazimuths near ~140°. This raises the possibility that this group of fast directions may result from sampling of structure farther to the east due to finite-frequency effects, discussed further below.

We repeated this exercise for the eastern stations (Figure 10, bottom row), although even the best-fitting model in this region does a poor job of fitting many of the observations. The eastern region model parameters of (–80°, 1.0 s) for the lower layer, and (60°, 0.4 s) for the upper layer are slightly different than for the mountain region, including a difference of 20° in fast direction for both the upper and lower layers. Although these two-layer models are not unique, this simple exercise does establish that a relatively slight change in model parameters in a two-layer anisotropic model can shift the predicted patterns of shear wave splitting (and its variation with backazimuth) enough to explain the qualitative differences in splitting behavior between the mountain and eastern stations (Figure 9). This helps to establish that a lateral change in anisotropy along the MAGIC line (particularly within the lithospheric mantle) represents a plausible explanation for the along-strike variability. Even the best-fitting two-layer models, however, cannot reproduce all of the details of the splitting patterns. This suggests that more than two layers are required to explain the observations, that finite frequency effects are important, that there is lateral heterogeneity within each region (particularly the eastern one) that cannot be modeled using our simplified approach, or a combination of these.

4.3. Contributions From Lithospheric Anisotropy and Implications for Lithospheric Deformation

The detailed view of lateral variations in upper mantle anisotropy beneath the MAGIC array afforded by our data set allows for new inferences on lithospheric and asthenospheric anisotropy, and thus past and present deformation, beneath the central Appalachian region. There are almost certainly contributions to splitting from both the mantle lithosphere and the asthenosphere beneath the MAGIC study area. We argue, however, that the sharp lateral transition in splitting patterns at the edge of the Appalachian Mountains most likely reflects laterally variable anisotropy in the lithospheric mantle; it is difficult to explain such a transition in terms of present-day flow in the asthenospheric mantle. This echoes the argument in Long et al. (2016) that lithospheric anisotropy makes a major contribution to the splitting pattern beneath the central and southern Appalachian Mountains. We emphasize, however, that the dense MAGIC station spacing at the eastern edge of the mountains allows us to resolve the sharp lateral contrast in splitting behavior, which we interpret as reflecting a sharp lateral contrast in lithospheric anisotropy, in detail. Finite-frequency sensitivity analysis of *SKS* phases with ~8–10 s period, such as those used in this study (e.g., Favier & Chevrot, 2003), suggests that our measurements should be sensitive to a mantle volume that has a width of roughly 100 km in the middle-upper mantle (e.g., Alsina & Snieder, 1995). This implies that stations located near the inferred lateral transition in the character of lithospheric anisotropy (that is, those located in eastern West Virginia and western Virginia) are likely sampling a combination of different anisotropic structures (e.g., Chevrot et al., 2004; Fischer et al., 2005). This interpretation is borne out by the histograms in Figure 5, which show that the mountain stations (third row, left plot) have a secondary peak in fast direction around

Figure 9. Variability in measured splitting parameters as a function of backazimuth for MAGIC and TA stations along the MAGIC line, divided regionally into (top row) western, (middle row) mountain, and (bottom row) eastern stations. Each individual measurement of (left plots) fast direction and (right plots) delay time are shown along with the 95% confidence region, and is plotted as a function of backazimuth modulo 180°. The backazimuths of null *SKS* arrivals are indicated with blue vertical bars. A roughly 90° periodicity with backazimuth is visible in the fast direction measurements for the mountain and eastern stations, suggesting multiple layers of anisotropy. Variability in measured fast directions is also evident, but the periodicity is less clear. In the western region, there is some variability in measured splitting parameters with backazimuth, but it is less dramatic than in the mountain and eastern regions.

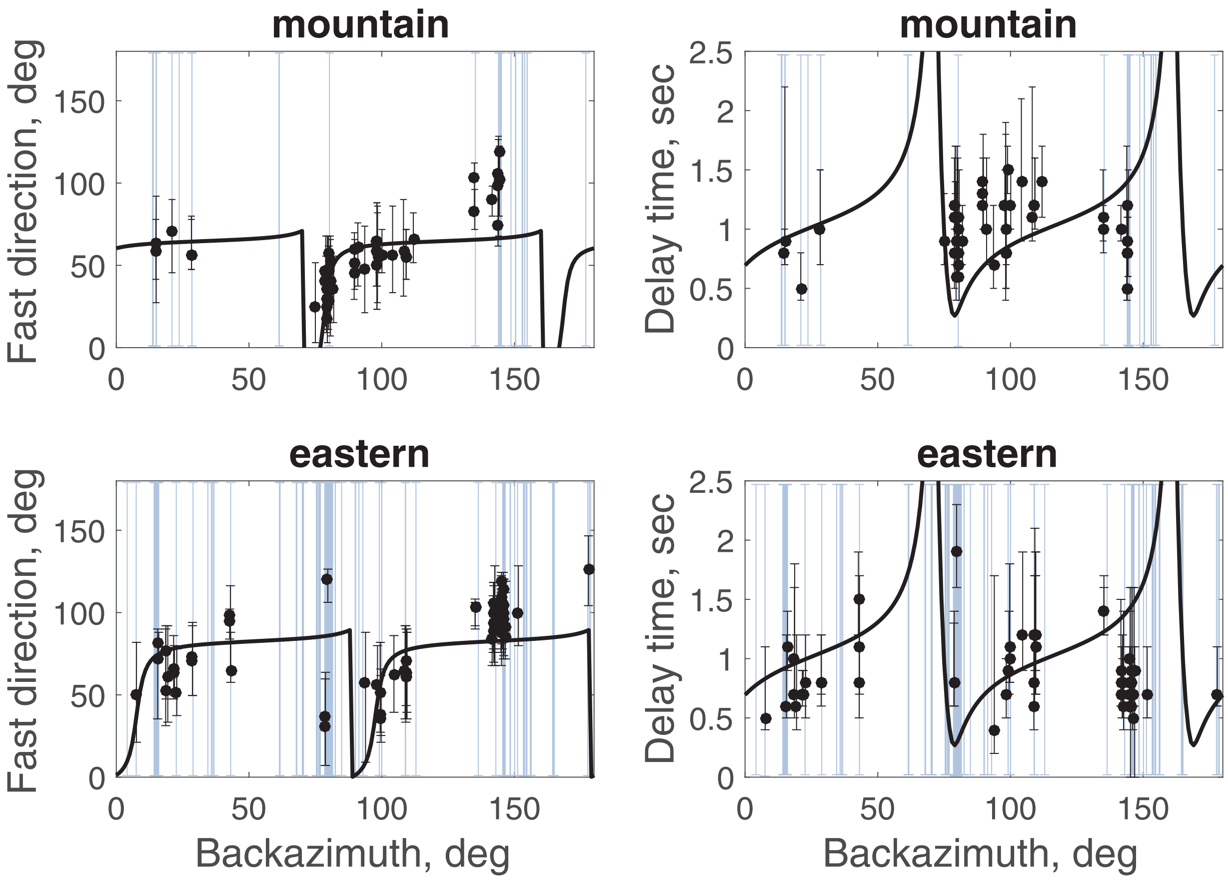

Figure 10. Results of simplified two-layer modeling beneath the mountain and eastern stations. (top plots) Apparent splitting parameters (left plot, fast directions; right, delay times) as a function of backazimuth beneath mountain stations, as in Figure 9. Black lines show the predictions for the best-fitting two-layer model, with parameters of (80°, 0.9 s) for the lower (asthenospheric) layer, and (40°, 0.3 s) for the upper (lithospheric) layer. (bottom plots) The same information for the eastern stations; here, the best-fitting model parameters are (–80°, 1.0 s) for the lower layer, and (60°, 0.4 s) for the upper layer.

100°. This may indicate some sampling of structure (due to finite frequency effects) beneath the eastern portion of the array, which is dominated by nearly E-W fast directions.

Although we favor a model that invokes lateral heterogeneity in lithospheric anisotropy to explain differences in splitting behavior along our array, we cannot totally rule out a scenario that invokes only present-day flow in the asthenosphere, if that flow is more complicated than horizontal, plate-motion-parallel shear. One particular scenario that may lead to lateral transitions in anisotropic geometry within the asthenosphere is edge-driven convection, which invokes small-scale convective flow at the edge of thick continental lithosphere (King, 2007; King & Anderson, 1998). Edge-driven convection has been invoked in the past as a potential explanation for shear wave splitting patterns beneath the southeastern U.S., particularly the region of the Coastal Plain that is dominated by weak or null *SKS* splitting (Long et al., 2010). It remains to be seen whether an edge-driven convection model can explain a lateral transition in splitting behavior as sharp as the one we have documented beneath our array. Ongoing modeling work as part of the MAGIC collaboration is currently testing models with realistic lithospheric geometries to understand whether this type of scenario represents a viable alternative to our preferred lithospheric anisotropy model.

One potential challenge to our model, in which lithospheric control is invoked as an explanation for lateral variations in splitting along the MAGIC array, is new evidence for relatively thin mantle lithosphere beneath the Central Appalachians. Unusually for a mature passive margin, our study area experienced volcanic activity at ~48 Ma, with the emplacement of magmatic rocks near present-day Harrisonburg, VA (Mazza et al., 2014). A lithospheric removal mechanism has been suggested as the most likely explanation for Eocene volcanism, based on geochemical arguments (Mazza et al., 2014, 2017). Recent results using USArray data have resolved a localized region of low seismic velocities in the upper mantle beneath Harrisonburg (e.g., Schmandt & Lin, 2014; Wagner et al., 2016), which may be consistent with lithospheric removal. Preliminary results along the MAGIC line from both magnetotelluric data and S-to-P receiver function analysis (Evans et al., 2016) are also consistent with thin lithosphere and suggest that the mantle lithosphere may be as thin as ~30 km beneath the "mountain" MAGIC stations. (The approximate region of inferred lithospheric loss and relatively low upper mantle seismic velocities is indicated on Figure 4c) An anisotropic layer of this thickness is unlikely to generate the ~1 s of *SKS* splitting we observe unless the anisotropy is unreasonably strong (up to ~14%), so an explanation that invokes anisotropy in the lithospheric mantle would require some combination of unusually strong lithospheric anisotropy, contributions from anisotropy within the middle to lower crust (e.g., Lin & Schmandt, 2014), or contributions from the asthenospheric mantle that interfere constructively with the lithospheric anisotropy signal. The crustal anisotropy model of Lin and Schmandt (2014), based on Rayleigh wave ellipticity measurements, exhibits generally orogen-parallel fast directions due to midcrustal anisotropy in our study region, so such a cumulative effect is plausible. We therefore envision a scenario in which the splitting we observe (and particularly the ~1 s delay times) reflects contributions from multiple layers of anisotropy via the cumulative effect of asthenospheric and lithospheric anisotropy. In this scenario, we attribute the observed lateral variations in splitting behavior to lateral variability in anisotropy (and thus past tectonic deformation) in the mantle lithosphere.

What does our inference of significant lithospheric contribution to *SKS* splitting patterns across the central Appalachians imply for lithospheric deformation associated with past tectonic processes? Our finding of generally orogen-parallel fast splitting directions beneath mountain stations is consistent with earlier results from the TA from Long et al. (2016), and are consistent with their interpretation that the mantle lithosphere underwent significant deformation during Appalachian orogenesis. This deformation was likely either in a pure shear geometry that aligns olivine fast axes parallel to the mountain belt, or had a component of lithosphere-scale transcurrent faulting (e.g., Barruol et al., 1997; Meissner et al., 2002; Silver & Chan, 1988; Tommasi & Vauchez, 2015; Vauchez & Nicolas, 1991). This deformation geometry may have been influenced by the geometric configuration of previous tectonic events such as the Grenville orogeny via tectonic inheritance (e.g., Vauchez & Barruol, 1996; Vauchez et al., 1997). Our inference of significant lithospheric deformation during Appalachian orogenesis is generally consistent with the idea of vertically coherent deformation (Silver, 1996) and suggests that the mantle lithosphere plays a key role in mountain building.

Our measurements likely also reflect some contribution from lithospheric deformation due to continental rifting, perhaps from multiple rifting episodes (including the both the late Proterozoic breakup of Rodinia and the Mesozoic breakup of Pangea). We note the spatial correspondence between the distinct lack of *SKS* splitting beneath MAGIC station PVGR and TA station P53A (Long et al., 2016) and the western edge of the Rome Trough, an Iapetan rift structure (e.g., Thomas, 2011). We speculate that this localized change in the splitting may be associated with lithospheric modification during rifting, although we note that MAGIC stations located within the Rome Trough (CDRF, ALMA, NAZF, and PETO) do not exhibit the same splitting behavior. There is no obvious explanation, however, for why Iapetan rifting may have affected the lithospheric structure only in a very localized region beneath the western edge of the Rome Trough; therefore, the connection between the null splitting beneath PVGR and P53A and past rifting processes remains speculative. Further to the east, the transition from generally NE-SW fast directions at mountain stations to more dominantly E-W directions at stations located just to the east (Figures 4 and 8) may reflect rifting-related overprinting of preexisting lithospheric anisotropy. We hypothesize that lithospheric extension that accompanied continental rifting associated with the breakup of Pangea during the Mesozoic may have overprinted the preexisting fabric beneath the Atlantic Coastal Plain (e.g., White-Gaynor & Nyblade, 2017). More work needs to be done, however, to fully understand to what extent and in what geometry the mantle lithosphere deforms during continental rifting episodes (e.g., Accardo et al., 2014; Eilon et al., 2014; Gao et al., 1997; Gashawbeza et al., 2004; Vauchez et al., 2000) under a range of conditions (for example, magma-poor versus magma-rich rifts; e.g., Kendall et al., 2006). A recent study of shear wave splitting beneath the Canadian Appalachians (Gilligan et al., 2016) argued for a limited contribution to lithospheric anisotropy from continental rifting processes, with only the Bay of Fundy and southern Nova Scotia exhibiting fast directions parallel to the inferred extension direction during the Mesozoic. Their inference of lithospheric anisotropy beneath the Canadian Appalachians that is mainly dominated by past deformation due to orogenesis, with localized modification of this signature due to later continental rifting, is similar to our findings beneath the MAGIC study area.

5. Summary

We examined lateral variations in *SKS* splitting along the dense MAGIC array across the central Appalachians, which traverses a variety of geologic units and topographic features. Our analysis reveals significant lateral variations in splitting behavior, along with complex splitting patterns that argue for contributions from multiple layers of anisotropy. We identify three distinct regions of anisotropic structure, based on measurements of (ϕ, δt) and the behavior of transverse component waveforms in record sections for individual events. Western stations are characterized by generally NE-SW fast directions and a large number of null *SKS* arrivals, with individual events exhibiting significant variability in transverse component waveform as along the array. Mountain stations exhibit far fewer null *SKS* arrivals and are dominated by orogen-parallel ϕ, consistent with previous studies based on TA data. There is a lateral transition in splitting behavior at the eastern edge of the Appalachian Mountains, with eastern stations exhibiting a considerably larger proportion of null arrivals and a distinct rotation of dominant fast directions to nearly E-W. There is compelling evidence for contributions to the observed splitting behavior from both the asthenospheric upper mantle and the lithosphere, as indicated by backazimuthal variations in splitting parameters, but the sharp transition in splitting behavior across the eastern edge of the Appalachians is likely controlled by shallow lithospheric anisotropy. We hypothesize that beneath the Appalachians, the mantle lithosphere was extensively deformed during Paleozoic orogenesis, while just to the east this lithospheric anisotropy signature was overprinted by later deformation associated with Mesozoic continental rifting.

Acknowledgements

Data supporting the conclusions in this paper can be found in supporting information Tables S1–S3. Seismic waveform data from the EarthScope USArray Transportable Array (network code TA) and the Mid-Atlantic Geophysical Integrative Collaboration (MAGIC) experiment (network code 7A) were accessed via the Data Management Center (DMC) of the Incorporated Research Institutions for Seismology (IRIS). The MAGIC deployment was supported by the EarthScope and GeoPRISMS programs of the National Science Foundation via grant EAR-1251515 to Yale University and grant EAR-1251329 to the College of New Jersey. The National Science Foundation I/D program helped support preparation of this manuscript. Any opinion, findings and conclusions or recommendations expressed in this article are those of the author and do not necessarily reflect the views of the National Science Foundation. The IRIS PASSCAL Instrument Center provided invaluable technical support during the MAGIC deployment. We are grateful to the many landowners and partner universities who hosted stations or provided logistical support for MAGIC and its pilot experiment, including Virginia Commonwealth University, Randolph-Macon College, College of William and Mary, James Madison University, West Virginia Wesleyan College, Glenville State College, Marietta College, Muskingum University, Denison University, and Ohio Northern University. We thank the many student volunteers who contributed to the MAGIC field effort. The Generic Mapping Tools (GMT; Wessel & Smith, 1999) and SACLAB utilities were used in this research. We thank Eric Kirby, Scott King, Shangxin Liu, and Scott Miller for helpful discussions. Finally, we are grateful to Mark Panning and an anonymous reviewer for insightful comments that improved this paper.

References

Accardo, N. J., Wiens, D. A., Hernandez, S., Aster, R. C., & Nyblade, A. (2014). Upper mantle siemsic anisotropy beneath the West Antarctic Rift System and surrounding region from shear wave splitting analysis. *Geophysical Journal of International*, *198*, 414–429. https://doi.org/10.1093/gji/ggu117

Alsina, D., & Snieder, R. (1995). Small-scale sublithospheric continental mantle deformation: Constraints from *SKS* splitting observations. *Geophysical Journal of International*, *123*, 431–448. https://doi.org/10.1111/j.1365-246X.1995.tb06864.x

Barruol, G., Silver, P. G., & Vauchez, A. (1997). Seismic anisotropy in the eastern United States: Deep structure of a complex continental plate. *Journal of Geophysical Research*, *102*, 8329–8348. https://doi.org/10.1029/96JB038000

Benoit, M. H., Ebinger, C., & Crampton, M. (2014). Orogenic bending around a rigid Proterozoic magmatic rift beneath the Central Appalachian Mountains. *Earth and Planetary Science Letters*, *402*, 197–208. https://doi.org/10.1016/j.epsl.2014.03.064

Buehler, J. S., & Shearer, P. M. (2017). Uppermost mantle seismic velocity structure beneath USArray. *Journal of Geophysical Research: Solid Earth*, *121*, 436–476. https://doi.org/10.1002/2016JB013265

Burton, W. C., Southworth, S. *et al*. (2010). A model for Iapetan rifting of Laurentia based on Neoproterozoic dikes and related rocks. In R. P. Tollo (Ed.) *From Rodinia to Pangea: The Lithotectonic record of the Appalachian region* (Geol. Soc. Am., Mem. 206, pp. 455–476). Boulder, CO: Geological Society of America. https://doi.org/10.1130/2010.1206(20)

Cawood, P. A., & Buchan, C. (2007). Linking accretionary orogenesis with supercontinent assembly. *Earth-Science Review*, *82*, 217–256. https://doi.org/10.1016/j.earscirev.2007.03.003

Chevrot, S. (2000). Multichannel analysis of shear wave splitting. *Journal of Geophysical Research*, *105*, 21579–21590. https://doi.org/10.1029/200JB900199

Chevrot, S., Favier, N., & Komatitsch, D. (2004). Shear wave splitting in three-dimensional anisotropic media. *Geophysical Journal of International*, *159*, 711–720. https://doi.org/10.1111/j.1365-246X.2004.02432.x

Darbyshire, F. A., Bastow, I. D., Forte, A. M., Hobbs, T. E., Calvel, A., Gonzalez-Monteza, A., & Schow, B. (2015). Variability and origin of seismic anisotropy across eastern Canada: Evidence from shear wave splitting measurements. *Journal of Geophysical Research: Solid Earth*, *120*, 8404–8421. https://doi.org/10.1002/2015JB012228

Deschamps, F., Lebedev, S., Meier, T., & Trampert, J. (2008). Stratified seismic anisotropy reveals past and present deformation beneath the east-central United States. *Earth and Planetary Science Letters*, *274*, 489–498. https://doi.org/10.106/j.epsl.2008.07.058

Diaz, J., Gallart, J., Villaseñor, A., Mancilla, F., Pazos, A., Córdoba, D., . . . Harnafi, M. (2010). Mantle dynamics beneath the Gibraltar Arc (western Mediterranean) from shear-wave splitting measurements on a dense seismic array. *Geophysical Research Letters*, *37*, L18304. https://doi.org/10.1029/2010GL044201

Eilon, Z., Abers, G. A., Jin, G., & Gaherty, J. B. (2014). Anisotropy beneath a highly extended continental rift. *Geochemistry Geophysics Geosystems*, *15*, 545–564. https://doi.org/10.1002/2013GC005092

Evans, R. L., Benoit, M. H., Long, M. D., Elsenbeck, J., & Ford, H. A. (2016). Evidence for lithospheric loss along the MAGIC line. In American Geophysical Union Fall Meeting, (Abstract T42D-07) AGU, San Francisco, CA.

Favier, N., & Chevrot, S. (2003). Sensitivity kernels for shear wave splitting in transverse isotropic media. *Geophysical Journal of International*, *153*, 213–228. https://doi.org/10.1046/j.1365-246X.2003.01894.x

Fischer, K. M., Li, A., Forsyth, D. W., & Hung, S.-H. (2005). Imaging three-dimensional anisotropy with broadband seismometer arrays. In A. Levander & G. Nolet (Eds.), *Seismic earth: Array analysis of broadband seismograms, Geophysical Monograph Series* (Vol. 157, pp. 99–116). Washington, DC: American Geophysical Union. https://doi.org/10.1029/157GM07

Fouch, M. J., Fischer, K. M., Parmentier, E. M., Wysession, M. E., & Clarke, T. J. (2000). Shear wave splitting, continental keels, and patterns of mantle flow. *Journal of Geophysical Research*, *105*, 6255–6275. https://doi.org/10.1029/1999JB900372

Fouch, M. J., & Rondenay, S. (2006). Seismic anisotropy beneath stable continental interiors. *Physics of the Earth and Planetary Interiors*, *158*, 292–320. https://doi.org/10.1016/j.pepi.2006.03.024

Gao, S., Davis, P. M., Liu, H., Slack, P. D., Rigor, A. W., Zorin, Y. A., . . . Logatchev, N. A. (1997). *SKS* splitting beneath continental rift zones. *Journal of Geophysical Research*, *102*, 22781–22797. https://doi.org/10.1029/97JB01858

Gashawbeza, E. M., Klemperer, S. L., Nyblade, A. A., Walker, K. T., & Keranen, K. M. (2004). Shear-wave splitting in Ethiopia: Precambrian mantle anisotropy locally modified by Neogene rifting. *Geophysical Research Letters*, *31*, L18602. https://doi.org/10.1029/2004GL020471

Gilligan, A., Bastow, I. D., Watson, E., Darbyshire, F. A., Levin, V., Menke, W., . . . Petrescu, L. (2016). Lithospheric deformation in the Canadian Appalachians: Evidence from shear wave splitting. *Geophysical Journal of International*, *206*, 1273–1280. https://doi.org/10.1093/gji/ggw207

Gripp, A. E., & Gordon, R. G. (2002). Young tracks of hotspots and current plate velocities. *Geophysical Journal of International*, *150*, 321–361. https://doi.org/10.1046/j.1365-246X.2002.0167.x

Hatcher, R. D. Jr. (2010). The Appalachian orogeny: A brief summary. In R. P. Tollo (Ed.), *From Rodinia to Pangea: The Lithotectonic Record of the Appalachian Region* (Geol. Soc. Am., Mem. 206, pp. 1–19). Boulder, CO: Geological Society of America. https://doi.org/10.1130/978-0-8137-1206-2

Hongsresawat, S., Panning, M. P., Russo, R. M., Foster, D. A., Monteiller, V., & Chevrot, S. (2015). USArray shear wave splitting shows seismic anisotropy from both lithosphere and asthenosphere. *Geology*, *43*, 667–670. https://doi.org/10.1130/g36610.1

Karato, S., Jung, H., Katayama, I., & Skemer, P. (2008). Geodynamic significance of seismic anisotropy of the upper mantle: New insights from laboratory studies. *Annual Review of Earth and Planetary Science*, *36*, 59–95. https://doi.org/10.1146/annurev.earth.36.031207.124120

Kendall, J.-M., Pilidou, S., Keir, D., Bastow, I. D., Stuart, G. W., & Ayele, A.(2006). Mantle upwellings, melt migration and the rifting of Africa: Insights from seismic anisotropy. In G. Yirgu (Ed.) *The Afar Volcanic Province with the East African Rift System Geological Society Special Publications* (Vol. 259, pp. 55–72). London, UK: The Geological Society of London.

Kennett, B. L. N., & Engdahl, E. R. (1991). Travel times for global earthquake location and phase identification. *Geophysical Journal of International*, *105*, 429–465. https://doi.org/10.1111/j.1365-246X.1991.tb06724.x

King, S. D. (2007). Hotspots and edge-driven convection. *Geology*, *35*, 223–226. https://doi.org/10.1130/G23291A.1

King, S. D., & Anderson, D. L. (1998). Edge-driven convection. *Earth and Planetary Science Letters*, *160*, 289–296. https://doi.org/10.1016/S0012-821X(98)00089-2

Levin, V., Menke, W., & Park, J. (1999). Shear wave splitting in the Appalachians and the Urals: A case for multilayered anisotropy. *Journal of Geophysical Research*, *104*, 17975–17993. https://doi.org/10.1029/1999JB900168

Li, Z. X., Bogdanova, S. V., Collins, A. S., Davidson, A., De Waele, B., Ernst, R. E., . . ., Vernikovsky, V. (2008). Assembly, configuration, and break-up history of Rodinia: A synthesis. *Precambrian Research*, *160*, 179–210. https://doi.org/10.1016/j.precamres.2007.04.021

Lin, F.-C., & Schmandt, B. (2014). Upper crustal azimuthal anisotropy across the contiguous U.S. determined by Rayleigh wave ellipticity. *Geophysical Research Letters*, *41*, 8301–8307. https://doi.org/10.1029/2014GL062362

Long, M. D., Benoit, M. H., Chapman, M. C., & King, S. D. (2010). Upper mantle seismic anisotropy and transition zone thickness beneath southeastern North America and implications for mantle dynamics. *Geochemistry, Geophysics, Geosystems*, *11*, Q10012. https://doi.org/10.1029/2010GC003247

Long, M. D., Gao, H., Klaus, A., Wagner, L. S., Fouch, M. J., James, D. E., & Humphreys, E. (2009). Shear wave splitting and the pattern of mantle flow beneath eastern Oregon. *Earth and Planetary Science Letters*, *288*, 359–369. https://doi.org/10.1016/j.epsl.2009.09.039

Long, M. D., Jackson, K. G., & McNamara, J. F. (2016). *SKS* splitting beneath Transportable Array stations in eastern North America and the signature of past lithospheric deformation. *Geochemistry, Geophysics, Geosystems*, *17*, 2–15. https://doi.org/10.1002/2015GC006088

Long, M. D., & Silver, P. G. (2009). Shear wave splitting and mantle anisotropy: Measurements, interpretations, and new directions. *Surveys in Geophysics*, *30*, 407–461. https://doi.org/10.1007/s10712-009-9075-1

Long, M. D., & Wiita, P. (2013). *Mid-Atlantic geophysical integrative collaboration*. International Federation of Digital Seismograph Networks, Seimic Network. Available at https://doi.org/10.7914/SN/7A_2013

Mazza, S. E., Gazel, E., Johnson, E. A., Bizimis, M., McAleer, R., & Biryol, C. B. (2017). Post-rift magmatic evolution of the eastern North American ''passive-aggressive'' margin. *Geochemistry, Geophysics, Geosystems*, *18*, 3–22. https://doi.org/10.1002/2016GC006646

Mazza, S. E., Gazel, E., Johnson, E. A., Kunk, M. J., McAleer, R., Spotila, J. A., . . . Coleman, D. S. (2014). Volcanoes of the passive margin: The youngest magmatic event in eastern North America. *Geology*, *42*, 483–486. https://doi.org/10.1130/G35407.1

McHone, J. G. (1996). Broad-terrane Jurassic flood basalts across northeastern North America. *Geology*, *24*, 319–322.

Meissner, R., Mooney, W. D., & Artemieva, I. (2002). Seismic anisotropy and mantle creep in young orogens. *Geophysical Journal of International*, *149*, 1–14. https://doi.org/10.1046/j.1365-246X.2002.01628.x

Miller, S. R., Sak, P. B., Kirby, E., & Bierman, P. R. (2013). Neogene rejuvenation of central Appalachian topography: Evidence for differential rock uplift from stream profiles and erosion rates. *Earth and Planetary Science Letters*, *369*, 1–12. https://doi.org/10.1016/j.epsl.2013.04.007

Polet, J., & Kanamori, H. (2002). Anisotropy beneath California: Shear wave splitting measurements using a dense broadband array. *Geophysical Journal of International*, *149*, 313–327. https://doi.org/10.1046/j.1365-246X.2002.01630.x

Powell, C. A., & Thomas, W. A. (2016). Grenville basement structure associated with the Eastern Tennessee seismic zone, southeastern USA. *Geology*, *44*, 39–42. https://doi.org/10.1130/G37269.1

Rowley, D. B., Forte, A. M., Moucha, R., Mitrovica, J. X., Simmons, N. A., & Grand, S. P. (2013). Dynamic topography change of the eastern United States since 3 million years ago. *Science*, *340*, 1560–1563. https://doi.org/10.1126/science.1229180

Rümpker, G., Ryberg, T., & Bock, G. and DESERT Seismology Group (2003). Boundary-layer mantle flow under the Dead Sea transform fault inferred from seismic anisotropy. *Nature*, *425*, 497–501. https://doi.org/10.1038/nature01982

Ryberg, T., Rümpker, G., Haberland, C., Stromeyer, D., & Weber, M. (2005). Simultaneous inversion of shear wave splitting observations from seismic arrays. *Journal of Geophysical Research*, *110*, B03301. https://doi.org/10.1029/2004JB003303

Schmandt, B., & Lin, F.-C. (2014). and S wave tomography of the mantle beneath the United States. *Geophysical Research Letters*, *41*, 6342–6349. https://doi.org/10.1002/2014GL061231

Silver, P. G. (1996). Seismic anisotropy beneath the continents: Probing the depths of geology. *Annual Review of Earth and Planetary Science*, *24*, 385–432. https://doi.org/10.1146/annurev.earth.24.1.385

Silver, P. G., & Chan, W. W. (1988). Implications for continental structure and evolution from seismic anisotropy. *Nature*, *335*, 34–39. https://doi.org/10.1038/335034a0

Silver, P. G., & Chan, W. W. (1991). Shear wave splitting and subcontinental mantle deformation. *Journal of Geophysical Research*, *96*, 16429–16454. https://doi.org/10.1o29/91JB00899

Silver, P. G., & Savage, M. K. (1994). The interpretation of shear-wave splitting parameters in the presence of two anisotropic layers. *Geophysical Journal of International*, *199*, 949–963. https://doi.org/10.1111/j.1365-246X.1994.tb04027.x

Thomas, W. A. (2011). The Iapetan rifted margin of southern Laurentia. *Geosphere*, *7*, 97–120. https://doi.org/10.1130/GES00574.1

Tommasi, A., & Vauchez, A. (2015). Heterogeneity and anisotropy in the lithospheric mantle. *Tectonophysics*, *661*, 11–37. https://doi.org/10.1016/j.tecto.2015.07.026

Vauchez, A., & Barruol, G. (1996). Shear-wave splitting in the Appalachians and the Pyrenees: Importance of the inherited tectonic fabric of the lithosphere. *Physics of the Earth and Planetary Interiors*, *95*, 127–138. https://doi.org/10.1016/0031-9201(95)03125-1

Vauchez, A., Barruol, G., & Tommasi, A. (1997). Why do continents break-up parallel to ancient orogenic belts? *Terra Nova*, *9*, 62–66. https://doi.org/10.1111/j.1365-3121.1997.tb00003.x

Vauchez, A., & Nicolas, A. (1991). Mountain building: Strike-parallel motion and mantle anisotropy. *Tectonophysics*, *185*, 183–201. https://doi.org/10.1016/0040-1951(91)90443-V

Vauchez, A., Tommasi, A., Barruol, G., & Maumus, J. (2000). Upper mantle deformation and seismic anisotropy in continental rifts. *Physics and Chemistry of the Earth*, Part A, *25*, 111–117. https://doi.org/10.1016/S1464-1895(00)00019-3

Wagner, L. S., Biryol, C. B., Fischer, K. M., & Hawman, R. B. (2016). Not so stable after all: Lithospheric structures beneath the southeastern United States. *Geological Society of America, Abstracts with Programs*, *48*, 202–206. https://doi.org/10.1130/abs/2016AM-288460

Wagner, L. S., Long, M. D., Johnston, M. D., & Benoit, M. H. (2012). Lithospheric and asthenospheric contributions to shear-wave splitting observations in the southeastern United States. *Earth and Planetary Science Letters*, *341*, 128–138. https://doi.org/10.1016/j.epsl.2012.06.020

Walker, A. M., & Wookey, J. (2012). MSAT – A new toolkit for the analysis of elastic and seismic anisotropy. *Computer & Geosciences*, *49*, 81–90. https://doi.org/10.1016/j.cageo.2012.05.031

Wessel, P., & Smith, W. H. F. (1999). Free software helps map and display data. *Eos. Transactions, American Geophysical Union*, *72*, 441–446. https://doi.org/10.1029/90EO00319

White-Gaynor, A. L., & Nyblade, A. A. (2017). Shear wave splitting across the Mid-Atlantic region of North America: A fossil anisotropy interpretation. *Geology*, *45*, 555–558. https://doi.org/10.1130/G38794.1

Wüstefeld, A., Bokelmann, G., Zaroli, C., & Barruol, G. (2008). SplitLab: A shear-wave splitting environment in Matlab. *Computer & Geosciences*, *34*, 515–528. https://doi.org/10.1016/j.cageo.2007.08.002

Yang, B. B., Liu, Y., Dahm, H., Liu, K. H., & Gao, S. S. (2017). Seismic azimuthal anisotropy beneath the eastern United States and its geodynamic implications. *Geophysical Research Letters*, *44*, 2670–2678. https://doi.org/10.1002/2016GL071227

Yuan, H., French, S., Cupillard, P., & Romanowicz, B. (2014). Lithospheric expression of geological units in central and eastern North America from full waveform tomography. *Earth and Planetary Science Letters*, *402*, 176–186. https://doi.org/10.1016/j.epsl.2013.11.057

Yuan, H., & Levin, V. (2014). Stratified seismic anisotropy and the lithosphere-asthenosphere boundary beneath eastern North America. *Journal of Geophysical Research: Solid Earth*, *119*, 3096–3114. https://doi.org/10.1002/2013JB010785

Yuan, H., & Romanowicz, B. (2010). Lithospheric layering in the North American craton. *Nature*, *466*, 1063–1068. https://doi.org/10.1038/nature09332